Stanford Exploration Project, Report 95, October 10, 1997, pages 1–264

Stanford Exploration Project, Report 95, October 10, 1997, pages 1–264

A theoretical comparison of equivalent offset migration and dip moveout prestack imaging

J. Bee Bednar [1]

keywords: *migration, DMO, prestack, imaging, time migration*

ABSTRACT

Equivalent-offset migration is a methodology for prestack-Kirchhoff time migration that partially reverses the order of velocity analysis, normal moveout correction, stack, and migration. Although claimed to be computationally and analytically superior to earlier time-domain approaches, it is not independent of velocity. Velocity-independent dip-moveout followed by prestack imaging is similar to equivalent-offset migration in that it also postpones normal moveout correction to the post-migration stage, but it is independent of velocity. In this paper, I investigate the theoretical relationship between these two processes, showing that equivalent-offset migration and prestack imaging are asymptotically equivalent. Moreover, equivalent-offset migration has little, if any, computational or analytic advantage. The fact that the combination of dip-moveout followed by prestack imaging is independent of velocity is a major advantage and suggests that this latter method is better suited to problems of velocity estimation.

INTRODUCTION

The purpose of seismic migration is accurate focusing of surface measurements at subsurface reflection points. Straight-ray limitations degrade the ability of time-migration techniques to produce accurate subsurface images. Relaxing constant velocity constraints by allowing velocities to vary as functions of midpoint and time does not resolve the issue. Rays are still forbidden to bend and, as a result, data are not properly focused.

Modern depth-imaging techniques allow rays to bend and are understood well enough to have become a standard part of data processing. They are rapidly leading to sophisticated methods for velocity estimation and mapping. One might conclude that further work on time based algorithms is unnecessary but depth migrations do have an Achilles heel. They require an acceptable initial velocity model prior to application. Without good initial velocity estimates, iterative depth migration can

[1]**email:** 71161.1260@compuserve.com, bednarb@sep.stanford.edu

lead to diasasterous results. Although estimation of prior velocity information is the subject of considerable discussion and research, approaches can be formulated to postpone velocity estimation until the data have been fully migrated.

The basic idea is to reverse the conventional processing sequence:

- Velocity Analysis (VA),
- Normal Moveout (NMO) Correction,
- Dip Moveout (DMO),
- Stack, (S) and
- Post-Stack Migration (PsSM)

to something like:

- Prestack Migration (PrSM),
- VA,
- Normal Moveout (NMO) Correction, and
- S.

In the latter approach, velocities are chosen after migration and so, in principle, are independent of dip. They are also estimated along image rays and, therefore, pertain more to true migrated positions than methods that do not incorporate migration in their formulation. A stacking-velocity field derived from migrated data provides an improved model for initial depth-imaging requirements.

There are several candidate techniques for reversing the processing sequence. Prestack-time-migration of normal-moveout-corrected common-offset sections followed by inverse NMO can be used to perform residual velocity analysis and in a sense provides a crude approach to the second processing sequence described above. Forel and Gardner (1988) develop a two-step dip-moveout (DMO) and prestack imaging (PSI) approach for forming common scatterpoint gathers. They claim that their method is completely velocity independent, and fully reverses the traditional processing sequence. Berryhill's (1996) non-imaging-shot-record migration is similar to Forel and Gardner's two-step approach and in fact M. Popovici (1994) claims that the two methods are equivalent. Moreover, Popovici (1994) shows that Berryhill's method is much faster computationally. This is an important issue for subsequent remarks and should be kept in mind as the paper progresses. The method described in (Ferber, 1994; Ferber et al., 1996) provides an additional approach to reversing the processing sequence, but is also similar in spirit to that of Forel and Gardner. Since it concentrates more on 3D issues it is of significant interest for that alone. Bancroft et al. (1994), (1995) introduced Equivalent-offset migration (EOM) suggesting that it is several orders of magnitude faster than more traditional Kirchhoff approaches. They claim (Bancroft, 1997; Bancroft et al., 1995; Bancroft and Geiger, 1994), that a major benefit of their method is the production of high fold, large offset common scatterpoint gathers that improve the focusing of velocity semblance resulting in improved velocity estimates. They suggest that rough initial velocity estimates are the only requirement for achieving this result. Bancroft (1997) further claims that the relationship between EOM and DMO followed by PSI (DMO-PSI) is superficial.

In view of the similarities, this paper contrasts the Forel and Gardner (1988) method with (Bancroft, 1997; Bancroft et al., 1995; Bancroft and Geiger, 1994) by first casting each within the same framework and notation. For the readers convenience, velocity-independent dip-moveout, prestack imaging, and equivalent-offset migration are each explained in separate sections using the same theoretical foundation. It is then clear that equivalent-offset migration only partially reverses the standard processing steps. The EOM schematic is VA, PrSM, NMO, and S. Moreover, EOM is asymptotically equivalent to the PSI step in DMO-PSI. On the other hand, dip-moveout followed by prestack imaging is a full reversal of the standard processing sequence. It is completely velocity independent. Both PSI and EOM perform the imaging step on constant time-slices by diffracting energy over appropriately defined curves. Not surprisingly, DMO can be implemented in exactly the same manner. The PSI curves are much simplier than those for EOM and so are significantly easier to implement. Although the details will not be discussed here, DMO-PSI can be formulated as a Fourier domain process and so has $O(n \log n)$ conputational complexity.

While all the results in this paper focus on 2D relationships, extension to 3D is straightforward.

THE VELOCITY INDEPENDENT DMO EQUATION

In the early 1980's G. H. F. Gardner and colleagues at the University of Houston showed that it was possible to DMO-correct recorded data in a velocity-independent manner. The fundamental basis for Gardner's method for velocity-independent DMO is the recognition that the double-square-root equation can be converted into a single-square-root equation by a radial-plane-diffraction process. After application of DMO, a second diffraction process, which takes place on constant time-slices completes the prestack migration step.

Consider a constant velocity medium with velocity v. With reference to Figure 1, the double-square root (DSR) equation is:

$$T = \sqrt{T_0^2 + \frac{(m - m_0 + h)^2}{v^2}} + \sqrt{T_0^2 + \frac{(m - m_0 - h)^2}{v^2}}. \tag{1}$$

Here m is the midpoint between source S and receiver R, m_0 is the arbitrary location of a fixed scatter point, h is the half-offset, T_0 is the one-way zero-offset traveltime from the normal to the constant-time ellipse at $(x = (m - m_0), y)$ to b, and T is the time required to traverse the path SPR. Note that in this case, both m_0 and m are referenced to the same fixed origin while $x = m - m_0$ is relative to m.

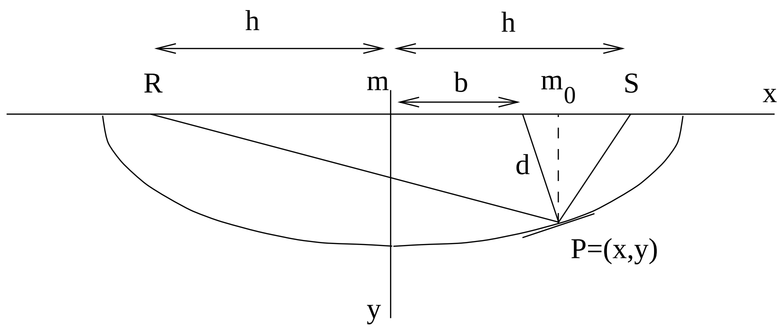

Figure 1: Depth section showing constant-time ellipse for the DSR equation. $\boxed{\text{bednara-Fig1}}$ [NR]

The ellipse in Figure 1 is the locus of all points (x, y) for which T is constant. It will be convenient to write (1) in the form:

$$T = \sqrt{T_0^2 + \frac{(x+h)^2}{v^2}} + \sqrt{T_0^2 + \frac{(x-h)^2}{v^2}}. \tag{2}$$

Following (Forel and Gardner, 1988), let

$$A = \frac{vT}{2}, \tag{3}$$

and

$$B = \sqrt{(A^2 - h^2)}. \tag{4}$$

Then

$$\frac{x^2}{A^2} + \frac{y^2}{B^2} = 1, \tag{5}$$

$$b = \frac{4xh^2}{v^2T^2}, \tag{6}$$

and the distance from b to P satisfies

$$d^2 = B^2(1 - \frac{b^2}{h^2}). \tag{7}$$

Since

$$d^2 = \frac{v^2T_0^2}{4} = (\frac{v^2T^2}{4} - h^2)(1 - \frac{b^2}{h^2}), \tag{8}$$

one has

$$T_0^2 = (1 - \frac{b^2}{h^2})T^2 - \frac{4h^2}{v^2}(1 - \frac{b^2}{h^2}) \tag{9}$$

This is the basic result from which DMO will be derived.

VELOCITY-INDEPENDENT DMO

Now define a new offset h_g and time T_1, as follows:

$$h_g^2 = h^2 - b^2, \tag{10}$$

and

$$T_1^2 = T_0^2 + \frac{4h_g^2}{v^2}. \tag{11}$$

Then after rearranging (9), one has

$$T_1 = \frac{h_g}{h} T, \tag{12}$$

Equations (10), (11), and (12) define velocity-independent DMO. They provide the framework for mapping traces with offset h and midpont m to zero-offset traces with offset h_g and midpoint $m + b$. Note that this process requires no velocity information and can be accomplished by a careful sampling or "binning" of b (Gardner, 1993). The trajectory of a single time sample T for a trace with half-offset h in the new offset space h_g is shown in Figure 2.

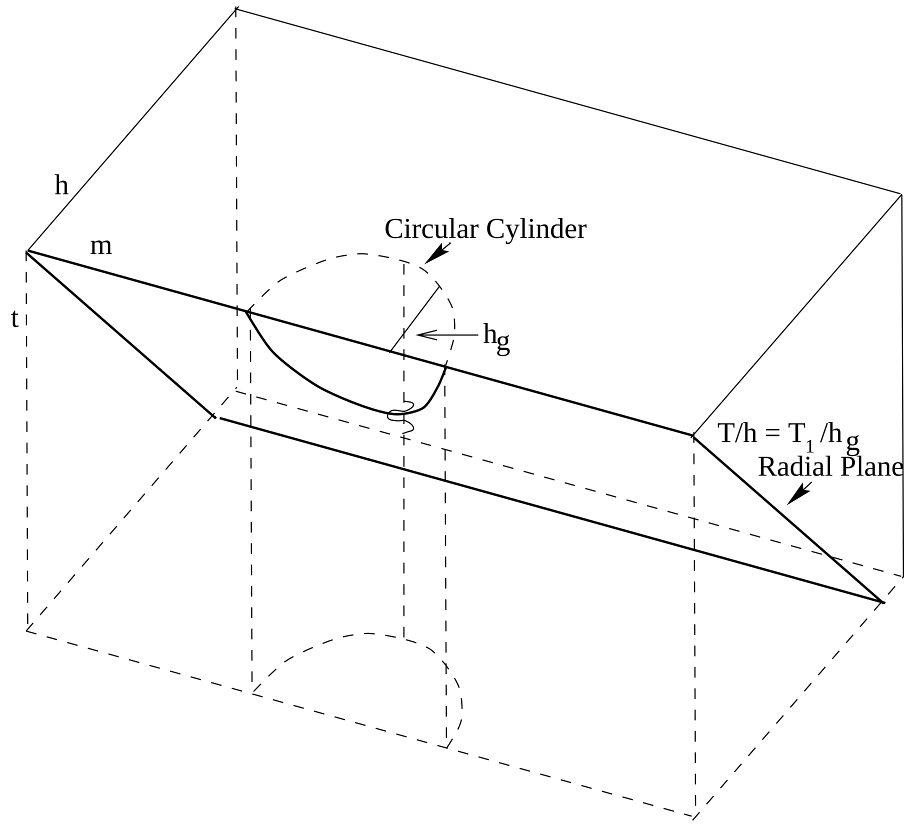

Figure 2: Radial-plane DMO. bednara-Fig2 [NR]

Each fixed sample in (m, h, t) space is mapped to a curve in $(m + b, h_g, t)$ space. Here, the curve lies in a radial plane, within the data volume (m, h, t), defined by

$h = \frac{h_g}{T_1}t$. It is possible to show (Gardner, 1993) that the mapping can be accomplished by (f, k) migration of the radial-plane data with the "velocity" $\frac{h_g}{T_1}$. Thus, the computational requirements for velocity-independent DMO are $O(n \log n)$. Although it is not within the scope of this article, Gardner (1993) also provides a log-stretch-(f, k) version of this DMO when h (common-offset section) is fixed.

After DMO, the new output volume consists of zero-offset but unmigrated data. Arrival times are specified by (11) and as a result are completely hyperbolic functions of h_g. The new data set can be NMO corrected, and stacked, to produce a zero-offset section. Any form of standard time migration may then be applied to produce a proper subsurface image.

Note also that if each new equivalent offset is migrated after NMO but prior to stack, then each point on the diffraction curve of Figure 2 will result in one of the circles indicated in Figure 3. After stack, the envelope of the circles, as also indicated in Figure 3, will be the equal-traveltime ellipse of (2). Since the radii of each of these circles is given by the velocity-independent equation (7), one can postulate that constant-velocity-prestack imaging requires no initial velocity information.

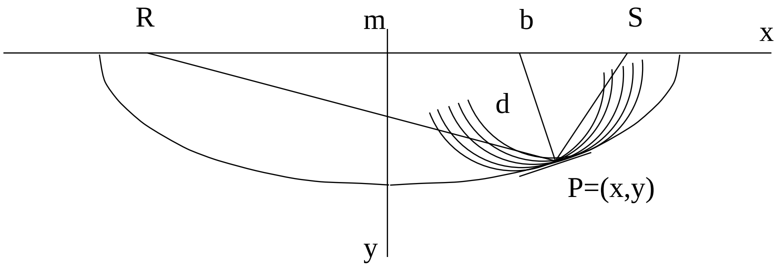

Figure 3: Ellipse as envelope of circles. bednara-Fig3 [NR]

VELOCITY-INDEPENDENT-PRESTACK IMAGING

At this point in the analysis, application of velocity-independent DMO has produced a volume with normal moveout given by

$$T^2 = T_0^2 + \frac{4((m - m_0)^2 + h^2)}{v^2} \tag{13}$$

Although one could, in principle, estimate v from this equation, the value would be relative to the normal from $m + b$ and not to the desired (migrated) location, m_0. To see what must be accomplished to migrate the DMO volume let

$$h_0^2 = (m - m_0)^2 + h^2. \tag{14}$$

The volume will be focused after points on the circle with center $(m_0, 0)$ and radius h_0 are mapped to the point (m_0, h_0). After focusing, the relation between T, T_0, h_0, and v is given by

$$T^2 = \sqrt{T_0^2 + \frac{h_0^2}{v^2}}. \tag{15}$$

Velocity-independent focusing requires that m_0 and h_0 be expressed in terms of m and h. First, differentiate (13) with respect to m and h to get

$$\frac{\partial T}{\partial m} = \frac{4(m - m_0)}{v^2 T}, \tag{16}$$

$$\frac{\partial T}{\partial h} = \frac{4h}{v^2 T}. \tag{17}$$

Second, solve for the derivative of h with respect to m

$$-\frac{\partial h}{\partial m} = \frac{\partial T/\partial m}{\partial T/\partial h} = \frac{(m - m_0)}{h}. \tag{18}$$

Finally, rewrite (18) as

$$m_0 = m + h\frac{\partial h}{\partial m}, \tag{19}$$

and substitute (19) into (14) so that

$$h_0^2 = h^2 + h^2(\frac{\partial h}{\partial m})^2. \tag{20}$$

Equations (19) and (20) define PSI. As illustrated in Figure 4, they transform constant T slices from variables (m, h) to variables (m_0, h_0). Clearly, there is no velocity dependence, so PSI is also a velocity-independent process. As was the case for DMO, PSI can also be formulated (Gardner, 1993) as an (f, k) process. In this case the process is equivalent to (f, k) (Stolt) modeling rather than migration.

EQUIVALENT OFFSET MIGRATION

Simple algebraic rationalization of (2) yields

$$T^2 = T_0^2 + \frac{h_e^2}{v^2}, \tag{21}$$

where

$$h_e^2 = x^2 + h^2 - \frac{4h^2x^2}{v^2T^2}, \tag{22}$$

is in fact the "equivalent-offset" formula of (Bancroft et al., 1995; Bancroft and Geiger, 1994).

As described by Bancroft et al. (1995), EOM is a PSI type process explained geometrically by Figure 5. The solid line in this figure represents the hyperbolic equivalent offset curve associated with the point (m, h, T) in the constant time-slice

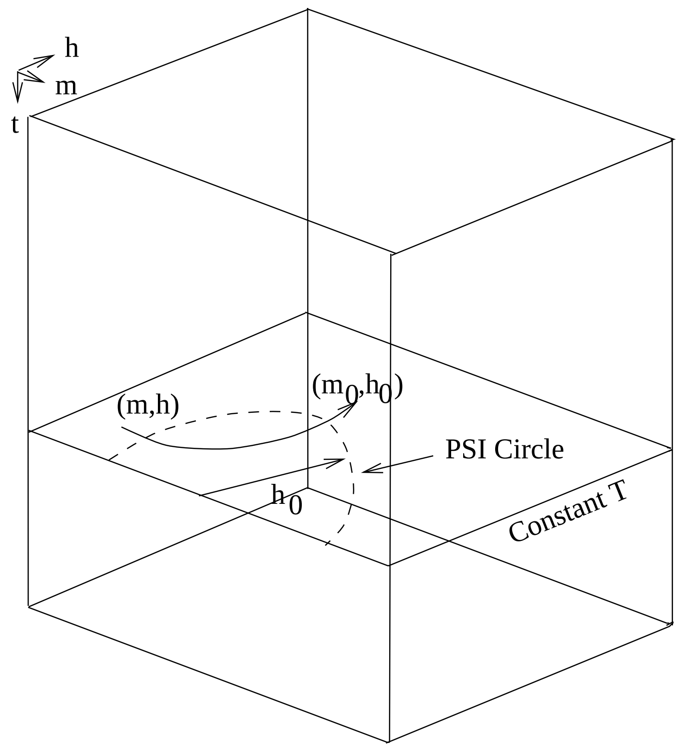

Figure 4: Prestack imaging for constant slice T. bednara-Fig4 [NR]

defined by T. The amplitude at time T on a trace with midpoint m and offset h is mapped to every point on this solid curve. Note that EOM is a diffraction-stack process so that each input point at constant time T and fixed offset h corresponds to a hyperbolic trajectory indexed by T with the new offset, h_e, varying as a function of equation (22). Computationally, the algorithm will have characteristics similar to those of standard prestack-Kirchhoff approaches. One can reduce the number of calculations by carefully limiting offset sampling, but the net result is an algorithm whose order is still proportional to n^3. That is, the number of calculations required to move input data is directly proportional to the number of points in the output volume, and so is of order n^3 for two-dimensional problems.

The presence of v^2T^2 in the denominator of (22) shows that EOM cannot proceed without knowledge or reasonable estimates of the velocity v. Clearly, the accuracy with which v is known has a direct and immediate bearing on the accuracy of the final migration. With the exception of the fact that residual NMO can improve the final image, one can expect the result of EOM to be basically similar to a good quality standard Kirchhoff migration.

To fully understand the similarities between EOM and DMO-PSI, one can attempt to follow the logic of equations (16), (18), (19), and (20). Repeating the exercise with

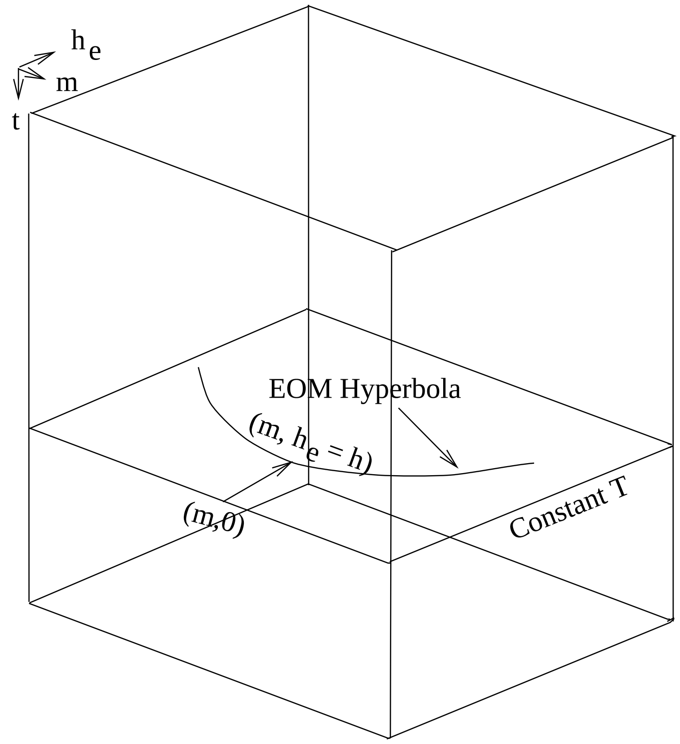

Figure 5: Equivalent-offset migration as a diffraction stack. bednara-Fig5 [NR]

(21) replacing (13) and $m_0 = m_e$ yields

$$\frac{\partial T}{\partial m} = 4(m - m_e)(1 - \frac{4h^2}{v^2T^2})(v^2T - \frac{4h^2x^2}{v^2T^3})^{-1}, \tag{23}$$

$$\frac{\partial T}{\partial h} = 4h(1 - \frac{4(m - m_e)^2}{v^2T^2})(v^2T - \frac{4h^2x^2}{v^2T^3})^{-1}, \tag{24}$$

and

$$-\frac{\partial h}{\partial m} = \frac{(m - m_e)}{h}(1 - \frac{4h^2}{v^2T^2})(1 - \frac{4(m - m_e)^2}{v^2T^2})^{-1}. \tag{25}$$

At first glance, the similarity of (25) with respect to (18) gives hope that EOM can be accomplished in the same manner as PSI. This is indeed true in theory. Equation (25) can be solved for $(m - m_e)$ via the standard formula for finding the roots of quadratic polynomials. Ignoring the obvious root-selection analysis that will have to be made, the resulting m_e can be substituted into (22) to specify h_e in terms of m and h. The two equations in m_e, and h_e could in theory be used in the same manner as (19) and (20). Unfortunately, no simple process for performing the indicated operations presents itself. One is still forced to use a diffraction stack methodology.

In the limit, as v^2T^2 approaches infinity, (25) becomes (18). Thus, EOM is asymptotically equivalent to PSI. Although beyond the scope of this paper, one is lead to consider the similarity between EOM and PSI in the absence of DMO and when each is followed by residual NMO. One might expect that for large v^2T^2, differences will be minor. In this case, errors in v will also be inconsequential, so the claim (Bancroft, 1997) of weak dependence on v is probably valid. On the other hand, the asymptotic equvalence of EOM and PSI suggest that when v^2T^2 is small, DMO-PSI will have an image-quality advantage.

Figures 4 and 6 summarize the basic similarities between EOM and PSI. The solid curves in these figures are the equivalent-offset hyperbola and the PSI circle. The dotted curve in Figure 6 schematically represents the locus of points (m, h, T) which map to (m_e, h_e, T), and is the equivalent of PSI's dotted circle in Figure 4. That is, the required amplitudes at (m_e, h_e) or (m_0, h_0) can be obtained either by diffracting along the solid curves or by summing over the dotted curves. In the limit, Figure 6 will become exactly equivalent to Figure 4. Conceptually, these processes are almost identical.

Since it is not obvious how to formulate EOM as (f, k) modeling, it is not clear that it can be implemented as an $O(n \log n)$ algorithm. The net impact is that the current best formulation of EOM on constant time slices is computationally equivalent to standard Kirchhoff migration techniques.

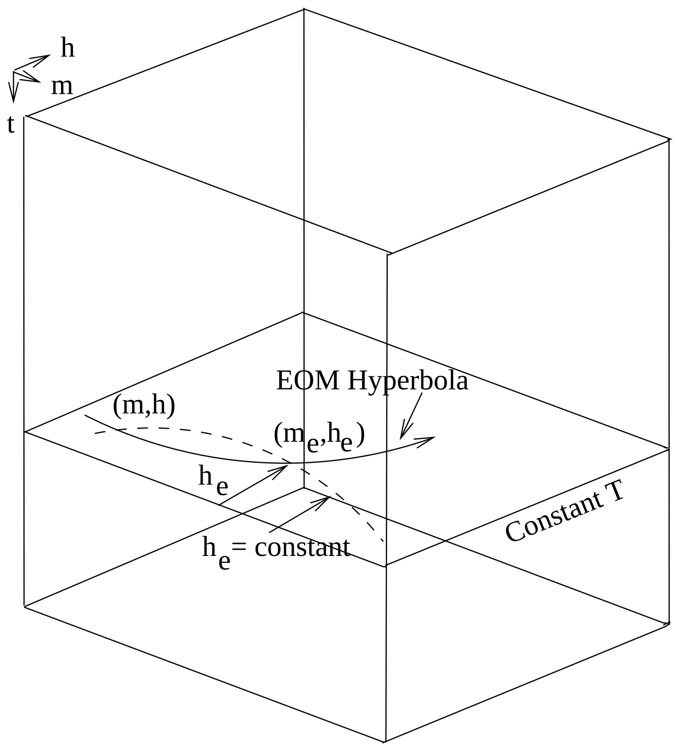

Figure 6: Equivalent-offset migration. $\boxed{\text{bednara-Fig6}}$ [NR]

CONCLUSIONS

Both equivalent-offset migration and dipmoveout-prestack imaging are prestack-time-migration techniques. While EOM is only a partial reversal of the standard processing sequence, DMO-PSI fully reverses the process and so is independent of velocity. EOM is shown to be conceptually and asymptotically identical to the PSI part of DMO-PSI. Both PSI and EOM perform the imaging step on constant time-slices by diffracting energy over appropriately defined curves. The PSI curves are much simpler than those for EOM and so are significantly easier to implement.

Theoretically, EOM is equivalent to PSI when the input data have been DMO corrected. In that case, the equivalent-offset formula for offset (h_e) as a function of midpoint, scatterpoint, velocity, v, and time, T, has no dependence on v^2T^2 and, the underlying curves are circles rather than hyperbolas. There are many alternative formulations of DMO-PSI, but the fact that the entire process can be completed in the frequency-wavenumber domain implies the existence of a very fast algorithm that is computationally superior to diffraction stacking.

Separation of prestack-constant-velocity migration into two steps, DMO and PSI, has an advantage over EOM in that it allows free choice of the DMO algorithm. The utilization of more sophisticated DMO techniques prior to PSI, e.g. Alfaraj and Larner (1992, 1991), ; Anderson and Tsvankin (1994); Anderson et al. (1994); Miller and Burridge (1989); Liner (1991, 1990), may improve both image quality and velocity estimates. Inclusion of reasonable isotropic velocity variations are possible in DMO-PSI. As anisotropic techniques mature it will also be possible to include anisotropic velocity variations in the imaging equation. This separability also allows one to apply a 3D DMO-PSI sequence followed by inverse 2D DMO to regularize irregular data sets and use 2D prestack-depth migration to achieve a 3D result (Canning and Gardner, 1993).

Velocity independence is definitely a powerful feature of any prestack technique. The inherent dependence of EOM on velocity estimates reduces its potential as a competitive alternative to DMO-PSI.

ACKNOWLEDGEMENTS

Jon Claerbout gets the award for providing the space, resources, and a great environment to do it. Thanks go to him, S. Fomel, and M. Prucha at SEP, and K. Larner at the Colorado School of Mines for keeping my wording ,spelling, and references honest. W. Symes at Rice, G. Neale in Tulsa, and N. Bleistein at the Colorado School of Mines are also acknowledged for supporting and encouraging completion of this work. Although he probably doesn't know it, P. Fowler showed me the relationship between the various techniques mentioned in the introduction.

REFERENCES

Alfaraj, M. and Larner, K., 1992, Transformation to zero offset for mode-converted waves (short note): Geophysics, **57**, no. 3, 474-477.

Alfaraj, M. and Larner, K., 1991, Dip-moveout for mode-converted waves: 61st Annual Internat. Mtg., Soc. Expl. Geophys., Expanded Abstracts, 1191-1193.

Anderson, J. E. and Tsvankin, I., 1994, Dip-moveout processing by Fourier transform in anisotropic media: 64th Annual Internat. Mtg., Soc. Expl. Geophys., Expanded Abstracts, 1213-1216.

Anderson, J. E., Alkhalifah, T. A., and Tsvankin, I., 1994, Fowler DMO and time migration in transversely isotropic media: 64th Annual Internat. Mtg., Soc. Expl. Geophys., Expanded Abstracts, 1217-1220.

Bancroft, J. C., 1997, A Review of Migration Fundamentals, in Hanson, D., Ed., Topics in Depth Imaging, Proceedings of the 1997 Spring Symposium of the Geophysical Scoiety of Tulsa, Society of Exploration Geophysicists, April 1, 1997.

Bancroft, J. C., Geiger, H. D., Foltinek, D., and Wang, S., 1995, Prestack migration by equivalent offsets and common scatter point (CSP) gathers: 57th Mtg. Eur. Assoc. Expl Geophys., Extended Abstracts, Session: P124.

Bancroft, J. C. and Geiger, H. D., 1994, Equivalent offset CRP gathers: 64th Annual Internat. Mtg., Soc. Expl. Geophys., Expanded Abstracts, 672-675.

Berryhill, J. R., System and method of seismic shot-record migration: U. S. Patent 5,544,126.

Miller, D., and Burridge, R., 1989, Multiparameter Inversion, Dip-moveout, and the Generalized Radon Transform, in Bednar, et. al., Eds, Geophysical Inversion, SIAM Proceedings in Applied Mathematics **52**.

Canning, A. and Gardner, G. H. F., 1993, Two-pass 3D prestack depth migration: 63rd Annual Internat. Mtg., Soc. Expl. Geophys., Expanded Abstracts, 892-894.

Ferber, R. G., Migration of muliple offset and velocity analysis, Geophysical Prospecting, **42**, 99-112.

Ferber, R. G., Sanders, B., and Yilmaz, O., Quick-look 3-D prestack time migration: 66th Annual Internat. Mtg., Soc. Expl. Geophys., Expanded Abstracts, 451-454.

Forel, D. and Gardner, G. H. F., 1988, A three-dimensional perspective on two-dimensional dip moveout: Geophysics, **53**, no. 5, 604-610.

Popovici, M., Berryhill's "pure-migration" = Gardner's PSI, Stanford Exploration Project, SEP-82.

Gardner, G. H. F., 1993, Three-dimensional seismic methods: Acquisition, processing and interpretation, Houston Advanced Research Center, The Woodlands, Texas.

Gardner, G. H. F. and Forel, D., 1990, Amplitude preservation equations for dip moveout (short note): Geophysics, **55**, no. 4, 485-487.

Liner, C. L., 1991, Born theory of wave-equation dip moveout: Geophysics, **56**, no. 2, 182-189.

Liner, C., 1990, General theory and comparative anatomy of dip moveout: Geophysics, **55**, no. 5, 595-607.